Brazilian Journal of Medical and Biological Research (1997) 30: 1033-1044
ISSN 0100-879X

Fast and slow voltage modulation of apical Cl^- permeability in toad skin at high $[K^+]$

J. Procopio

Departamento de Fisiologia e Biofísica, Instituto de Ciências Biomédicas, Universidade de São Paulo, 05508-900 São Paulo, SP, Brasil

Abstract

The influence of voltage on the conductance of toad skin was studied to identify the time course of the activation/deactivation dynamics of voltage-dependent Cl^- channels located in the apical membrane of mitochondrion-rich cells in this tissue. Positive apical voltage induced an important conductance inhibition which took a few seconds to fully develop and was instantaneously released by pulse inversion to negative voltage, indicating a short-duration memory of the inhibiting factors. Sinusoidal stimulation at 23.4 mM $[Cl^-]$ showed hysteresis in the current versus voltage curves, even at very low frequency, suggesting that the rate of voltage application was also relevant for the inhibition/releasing effect to develop. We conclude that the voltage modulation of apical Cl^- permeability is essentially a fast process and the apparent slow components of activation/deactivation obtained in the whole skin are a consequence of a gradual voltage build-up across the apical membrane due to voltage sharing between apical and basolateral membranes.

Correspondence
J. Procopio
Departamento de Fisiologia
e Biofísica, ICB, USP
Av. Prof. Lineu Prestes, 1524
05508-900 São Paulo, SP
Brasil

Research supported by FAPESP, CNPq and Blue Life.

Received August 1, 1996
Accepted June 30, 1997

Key words
- Cl^- channel
- Toad skin
- Voltage modulation
- Epithelia

Introduction

It is known that hyperpolarization of toad skin epithelium leads to a slow activation of a Cl^- conductive pathway (1-12). Models based on slow voltage activation of apical Cl^- channels have been proposed in order to explain this observation (5,7,9). Also, there is ample evidence that Cl^- ions move through a specialized cell compartment consisting of the mitochondrion-rich cells (MR-cells) (1,2,13-15). Evidence for voltage modulation was investigated by us (10,16; Procopio J, unpublished data) with the conclusion that Cl^- permeability in the apical membrane of the Cl^- transporting cells is not exclusively dependent on voltage, but requires additional presence of Cl^- ions in either the external solution or in the cytoplasm (10,16-18). The exact role of cytoplasmic Cl^- ions in the modulation of apical Cl^- permeability is still unknown. Experimental evidence suggests that a minimum concentration of Cl^- ions in the cytoplasm and external solution is a necessary condition for the activation of apical Cl^- permeability (12,18). In favor of this idea is the fact that all maneuvers eliciting Cl^- permeability in the skin are associated with states in which cytoplasmic $[Cl^-]$ is presumably higher than normal. For example, the well-known Cl^- permeability activation achieved by hyperpolarizing the skin in NaCl Ringer solution (9) creates a condition for both apical depolarization and Cl^- entry into

the MR-cells. In this case, coincidentally, conductance activation is slow and sigmoidal in time, indicating a previously quiescent Cl^- permeability.

Another unanswered question is the time course of Cl^- permeability activation/inhibition by voltage. Studies pioneered by Larsen (9) have concluded that activation of apical Cl^- permeability by voltage is an intrinsically slow process, keeping pace with the temporal course of the experimentally measured current evolution after voltage changes. As such, after a voltage step, current activation develops in a sigmoidal fashion, with a time course measured in fractions of a minute. This is in clear contrast to most of the voltage-activated channels which have been described and which have activation kinetics measured in milliseconds.

Recent results of Larsen and Harvey (19) measuring individual whole MR-cell currents do not entirely answer this question and provide further evidence for a voltage dependence of apical Cl^- channels. The slow activation/deactivation kinetics of apical Cl^- permeability (P_{Cl}) observed in the whole skin cannot be explained in terms of the much faster kinetics seen in individual MR-cells.

A problem that seriously limits the interpretation of such experimental results in amphibian skin is the existence of 2 functional barriers in series, namely the apical and basolateral membranes of the MR-cells (Figure 1).

The aim of the present study was to investigate the voltage dependence of the apical Cl^- pathway under conditions of high $[K^+]$ Ringer, in which the basolateral membrane of the Cl^--transporting cells is presumably depolarized to a high extent and rendered considerably more conductive (20). Under the above conditions, and in the presence of a transepithelial short circuit, it is expected that the apical membrane will also importantly depolarize in the presence of symmetrical KCl Ringer. Additionally, as a consequence of the small cell negativity brought about by this condition, cytoplasmic $[Cl^-]$ should be considerably higher as compared to the condition of symmetrical NaCl Ringer usually employed in previous studies (9).

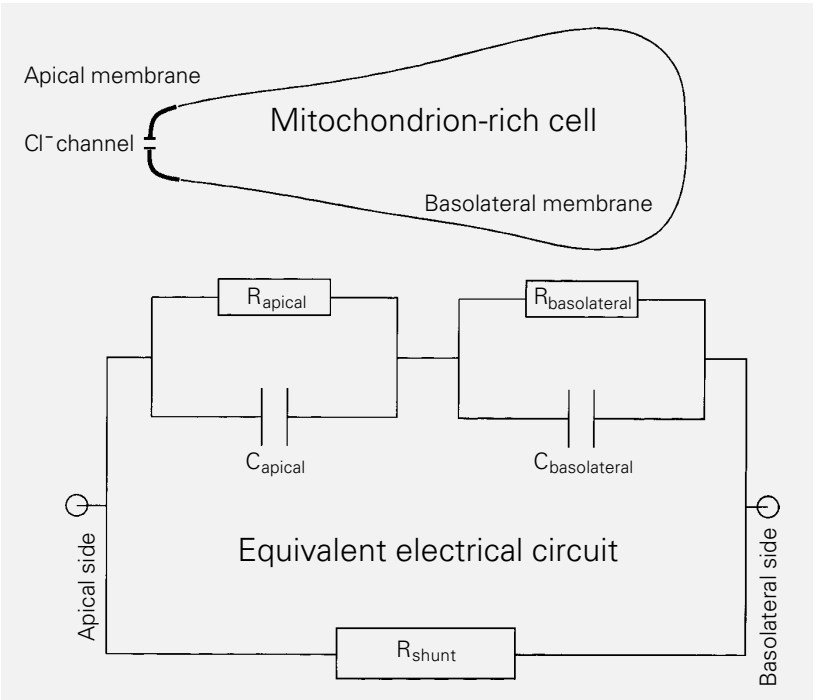

Figure 1 - Mitochondrion-rich cell and its equivalent electrical circuit. *Top*, Schematic representation of a mitochondrion-rich cell (MR-cell) of the epithelium, indicating the locations of the apical and basolateral membranes and of apical voltage-dependent Cl^- channels. *Bottom*, Equivalent electrical circuit of the MR-cell compartment. The voltage-dependent Cl^- channels are located on the apical membrane. Electromotive forces were taken out for simplification. R_{apical} and $R_{basolateral}$ are the apical and basolateral resistances, respectively. C_{apical} and $C_{basolateral}$ are the apical and basolateral capacitances, respectively. R_{shunt} is the resistance of the shunt-pathway which in our case essentially includes the paracellular space and the principal cell compartment.

Material and Methods

Toads of the species *Bufo marinus ictericus* were employed. The animals were kept under fasting condition with free access to running tap water. Skins were removed after double-pithing the animals and carefully testing for the absence of pain reflexes, mounted and studied within 6 h after animal death.

A model DVC-1000, 4-electrode voltage/current clamp (World Precision Instruments, New Haven, CT) was employed both to clamp the voltage and to measure the current through the skin. Current was passed by means of Ag/AgCl electrodes embedded into conductive agar plugs. Voltage was probed with 3 M KCl agar bridges connected to calomel half-cells.

The polarity of the voltage pulses is that of the apical side, with the serosal side bath taken as zero reference level. Current responses were recorded/acquired by means of an analog/digital Labmaster type interface and fed to a PC type computer with the help of the Axotape v.2 program (Axon Instruments Inc., Foster City, CA), at a sampling rate of 1 kHz. Skin fragments measuring 1.13 cm^2 were mounted vertically between two identical Lucite, Ussing-type hemi-chambers. A special recess of the rim, filled with vacuum grease, minimized the effect of edge damage. Solutions were vigorously stirred by means of independent mixers. The current sign convention is such that current passing in the apical to serosal direction is considered to be positive.

Solutions without sodium contained 117 mM $[K^+]$ (as $KHCO_3$ and KCl or K_2SO_4), 1 mM $[Ca^{2+}]$ (as $CaCl_2$ or $CaSO_4$) and 2.5 mM $[HCO_3^-]$ (as $KHCO_3$), pH = 8.2 after aeration. Chloride concentration was variable, with Cl^- being replaced with SO_4^{2-}. Three concentrations of Cl^- were used: 100% KCl Ringer ($[Cl^-]$ = 117 mM), 20% KCl Ringer ($[Cl^-]$ = 23.4 mM) and sulfate K^+ Ringer ($[Cl^-]$ = 0). Symmetrical solutions were employed in all experiments. In sinusoidal voltage stimulation the sinoids were generated by a digital Hewlett Packard 3245A Universal Source Wave Generator.

The experimental design did not permit statistical analysis based on mean and standard deviation. Average curves were tentatively produced but it was found that this considerably blurred the data. A total of 6 skins were studied in the pulse protocols and 4 skins in the sinusoidal stimulation. All skins were found to respond in essentially the same way and typical records for each experimental group are presented. Figure 1 schematically illustrates the skin elements relevant to the present study.

Results

The current response to high amplitude negative pulses (100 mV) in 20% Cl^- Ringer was characterized by a triphasic time course consisting of an ohmic response followed by a small and fast decay and, finally, a slow activation of small importance (not apparent in the present record), developing within the first few seconds (Figure 2A). Voltage clamping to zero after conditioning at negative apical voltages invariably generated a tail current (hereafter called *relaxation current*).

With $[Cl^-]$ = 0 there was always a transient and very fast overshoot of current in response to negative (Figure 2D) voltage transitions, followed by a small but consistent oscillation of the current. The complete transient lasted no more than 40 ms. The response to positive pulses is a mirror image of Figure 2D. The life-time of this transient appeared to increase with increasing Cl^- concentration, whereas its relative amplitude decreased with increasing $[Cl^-]$ until its disappearance in 100% Cl^- Ringer (Figure 2C).

Current (I) *vs* voltage (V) relations were obtained under three experimental conditions regarding Cl^- concentration: 0%, 20% and 100% in relation to the pure Cl^- Ringer having $[Cl^-]$ = 117 mM.

In 100% Cl^- Ringer (Figure 3A), currents measured at 20 ms did not differ from those measured at later times and the I *vs* V relation was a straight line crossing the zeros.

In 20% Cl^- Ringer (Figure 3C), the "instantaneous" (at 20 ms) current *vs* voltage relation was essentially a straight line crossing the zeros. Currents measured at later times (40 to 1000 ms) indicated a progressive rectification in the positive voltage range.

After prolonged negative pulses were clamped back to zero, both the instantaneous amplitude (data not shown) and the area under the relaxation currents (equivalent to an amount of electrical charge) increased with the duration of the negative pulse, as shown in Figure 3D. Small relaxation currents were also found following positive voltage pulses (data not shown).

In 0% Cl^- Ringer (Figure 3B) the I *vs* V relations were measured at 8 ms, the peak of the current response, and at 20 ms, the steady-state values. Both relations were straight lines but the currents measured at 8 ms were significantly higher than those measured at 20 ms. Since the current transient was very short compared to those at 20% or 100% Cl^- Ringer the sharp peaks observed at 8 ms were probably capacitive transients.

The current response to positive apical pulses (in 23.4 mM [Cl^-]) was different from the response to negative pulses: a fast deflection of the same amplitude as that seen in response to negative voltages (see I *vs* V relations) was followed by a fast and very marked decline of the current (Figure 2B). The large current inactivation that followed the positive pulse in 23.4 mM [Cl^-] became much less important in going to 117 mM [Cl^-] (Figure 2C) or to zero [Cl^-] (data not shown).

Upon clamping to zero after positive apical pulses there was also a small relaxation current of negative direction and smaller in amplitude than that following negative pulses. This current might reflect a fast entry of Cl^- into cells that were previously depleted of Cl^- ions by the conditioning period at high positive apical voltages. In the case of positive pulse clamping to zero, however, the apical membrane was presumably less permeable to Cl^- due to the previous conditioning at positive apical voltage, a fact which explains the smaller relaxation current.

In a second type of protocol the skin was

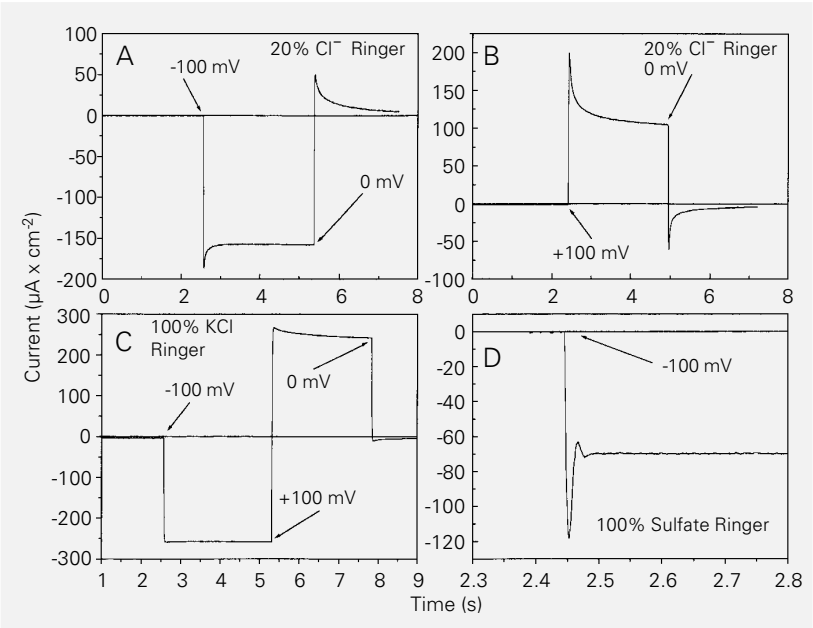

Figure 2 - Response of the skin to voltage steps. *A*, Current response to voltage steps in the subsecond and few second time range in symmetrical KCl Ringer with [Cl^-] = 23.4 mM with the voltage sequence 0 → -100 mV → 0 mV. *B*, Same solution as in A and voltage program 0 mV → +100 mV → 0 mV. *C*, Current responses to voltage pulses in symmetrical KCl Ringer with [Cl^-] = 117 mM. Voltage sequence is 0 mV → -100 mV → +100 mV → 0 mV. *D*, In zero [Cl^-] Ringer (symmetrical) with voltage sequence 0 mV → -100 mV (response to 0 → +100 mV is mirror image).

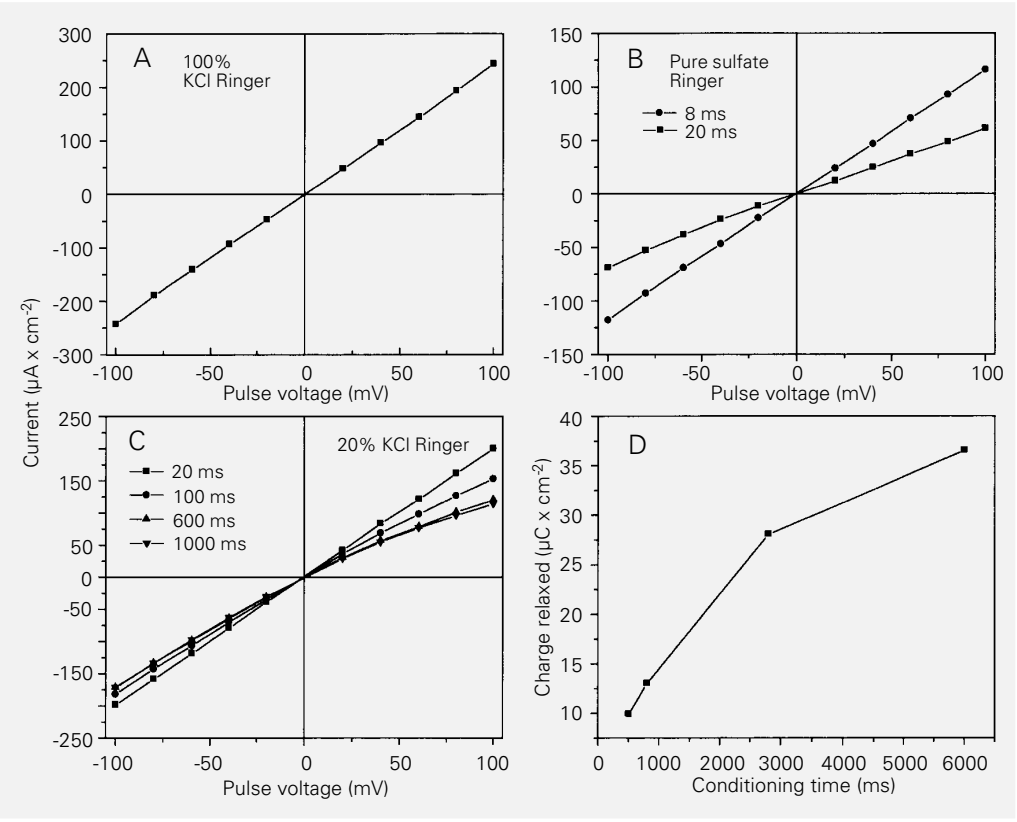

Figure 3 - Current *vs* voltage relations in symmetrical KCl Ringer and relationship between pulse duration and integral of tail current. *A*, $[Cl^-]$ = 117 mM, recorded after 20 ms. *B*, $[Cl^-]$ = 0, recorded at 8 and 20 ms. *C*, $[Cl^-]$ = 23.4 mM, recorded at different time intervals from pulse to register, indicated in the curves. *D*, Relation between relaxation currents (integral area) and pulse duration (clamping to zero from -100 mV).

conditioned for a given period at a negative or positive apical voltage of 100 mV and then clamped directly to the opposite voltage of the same amplitude.

The current response to directly stepping from -100 to +100 mV in 20% Cl^- Ringer (Figure 4A) had an instantaneous component which was invariably higher than the response to clamping from zero to -100 mV or from zero to +100 mV, by a factor of about 1.5.

The current response to directly clamping from +100 to -100 mV in 20% Cl^- Ringer was considerably different from that observed with the opposite maneuver (Figure 4B); despite a pronounced inhibition of the current after a few seconds of conditioning at +100 mV the instantaneous current response to directly stepping to -100 mV was identical to that observed as a response from zero to either -100 or +100 mV. Apparently, the "memory" of the previous conditioning at +100 mV was virtually nil in the sense that the inhibitory effect of a positive pulse on the current was instantaneously released upon inverting the voltage.

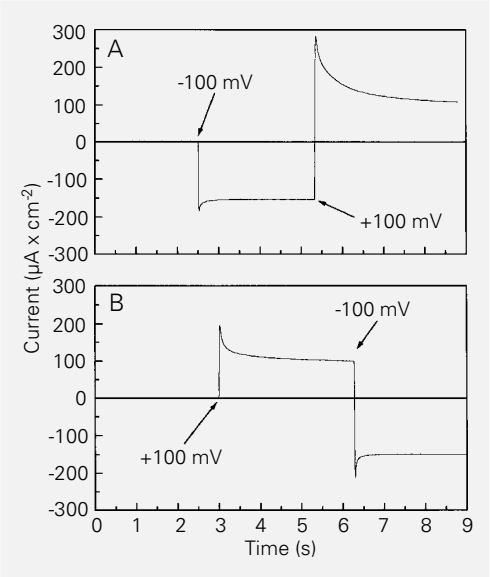

Figure 4 - Voltage pulse combinations. Solutions are symmetrical KCl Ringer with $[Cl^-]$ = 23.4 mM. In *A* the voltage sequence is 0 → -100 mV (about 3 s) → +100 mV (about 4 s). In *B* the sequence is 0 → +100 mV (about 4 s) → -100 mV (about 4 s).

The current *vs* voltage characteristics of the skin stimulated by sinusoidal voltages were studied at frequencies between 0.02

and 1 Hz, which constituted relatively fast dV/dt sweeps but at a rate slow enough to prevent significant contamination with capacitive currents, allowing also for enough time for the activation and inhibition of apical Cl^- permeability to develop.

Current *vs* voltage curves were obtained under three experimental conditions regarding Cl^- concentration in the bathing solutions (in that sequence): 20% Cl^- Ringer, 0% Cl^- Ringer and 100% Cl^- Ringer.

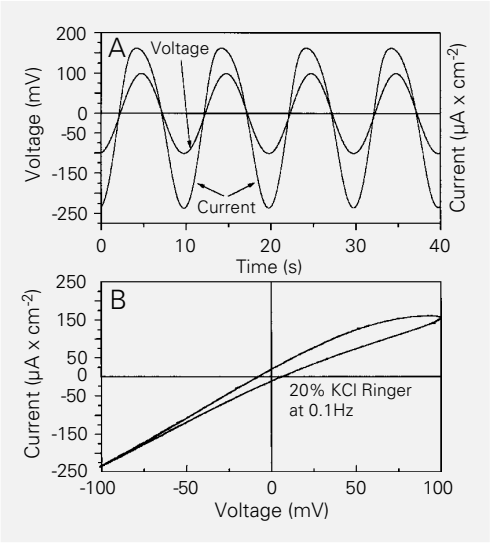

Figure 5 - Response to sinusoidal voltages at 0.1 Hz and [Cl^-] = 23.4 mM. *A*, Applied voltage and corresponding current response are plotted against time in symmetrical KCl Ringer with [Cl^-] = 23.4 mM, at frequency = 0.1 Hz. Clear deviation from a pure resistive response is observed. *B*, Same data as in *A*, but with current plotted against voltage. Hysteresis is clearly seen.

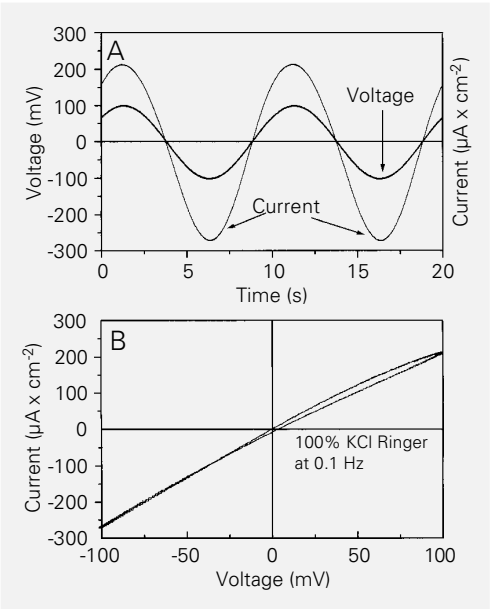

Figure 6 - Response to sinusoidal voltage at 0.1 Hz and [Cl^-] = 117 mM. *A*, Applied sinusoidal voltage and current response of the skin plotted against time in symmetrical KCl Ringer with [Cl^-] = 117 mM and frequency of 0.1 Hz. *B*, Current and applied voltage of *A* plotted against each other.

Figure 5A shows both current and voltage as a function of time, in 20% Cl^- Ringer at 0.1 Hz. Despite no large phase difference, it can be easily observed that the current curve is not symmetrical in time.

Figure 5B is constructed with the same data as Figure 5A, but with the current plotted as a function of voltage. In order to describe the I *vs* V relations we assumed each cycle as beginning at V = -100 mV then going to +100 mV and then back to -100 mV. The plots were generated in a clockwise direction. As such we define an *ongoing* phase from -100 to +100 mV and a *returning* phase from +100 to -100 mV. The following points are to be noted in Figure 5B: 1) There was pronounced rectification at positive voltages on both ongoing and returning legs. 2) The ongoing leg of the curve did not coincide with the returning leg. The lack of a large phase difference between current and voltage (the extreme values of current and of voltage coincide on both extremes) suggests that the contribution of the capacitive impedance is minimal up to this frequency. As such, the existence of different pathways for the ongoing and returning legs on the I *vs* V figure points to a *hysteresis effect*, i.e., at a given voltage, the electrical resistance of the skin in the ongoing phase of the curve differs from that at the returning phase. It can be easily noticed that the hysteresis was more marked in the positive voltage range, as expected from previous observations showing that positive apical voltages inhibit Cl^- permeability. 3) The I *vs* V figures obtained in consecutive cycles exactly overlapped (data not shown). 4) The returning leg of the I*vs* V curve resembled the instantaneous I *vs* V relations obtained with the voltage pulse experiments at 200-600 ms.

As the frequency of the sinusoidal stimulation increased to 1 Hz hysteresis intensified and invaded also the negative voltage side of the curve. This raises the possibility that, at higher frequencies, capacitive impedance might be playing a role, although a

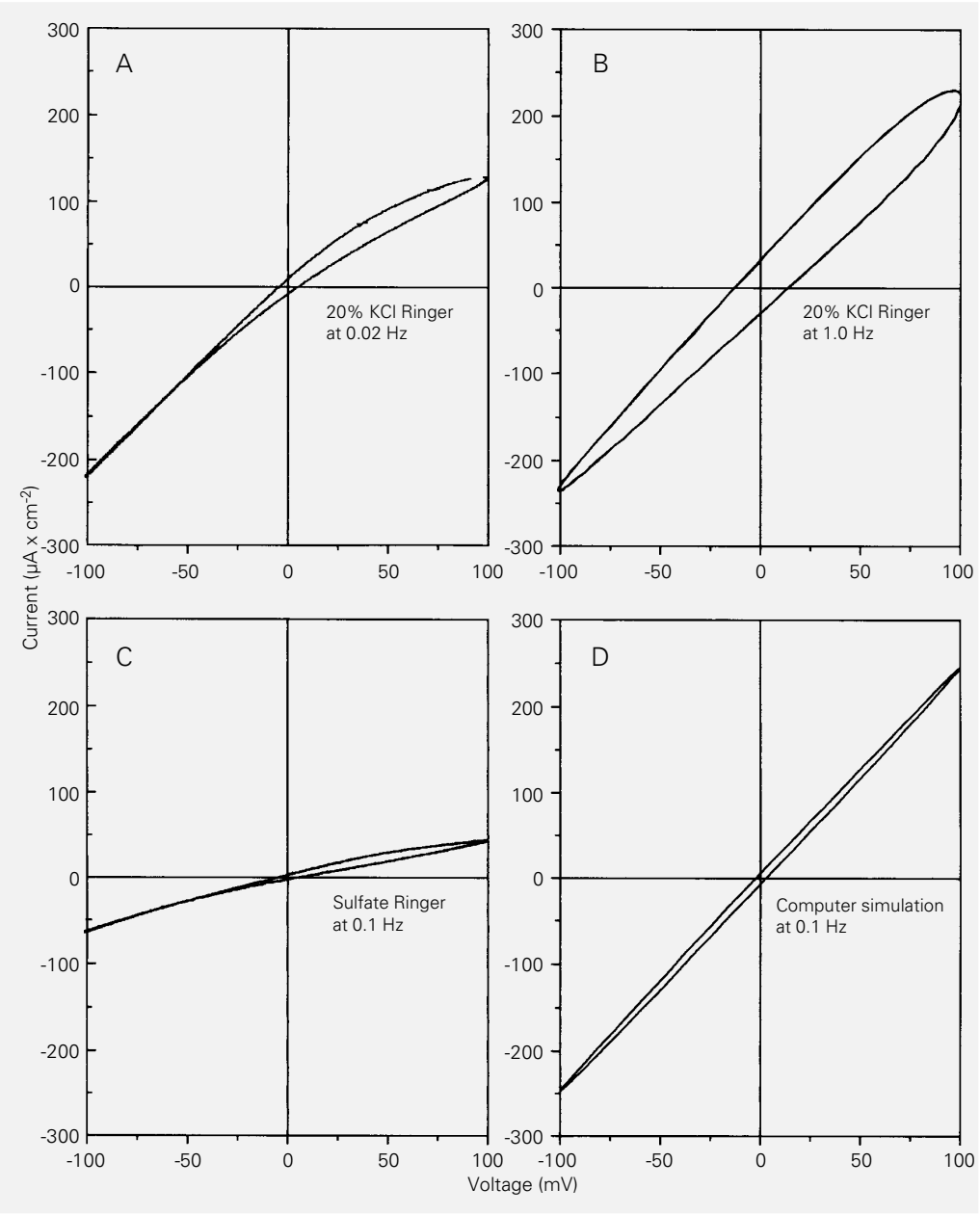

Figure 7 - Response to sinusoidal voltages under other conditions. *A*, I *vs* V relation with sinusoidal stimulation at 0.02 Hz and 20% Cl^- Ringer. *B*, Same protocol as in *A*, but stimulation at 1.0 Hz. *C*, I *vs* V relation with 0.1 Hz sinusoidal stimulation in pure sulfate (absence of Cl^-) Ringer. *D*, Computer simulation of the current *vs* voltage relation for a parallel RC circuit with R = 406 ohm (typical skin resistance in 20% Cl^- Ringer) and C = 100 microFarad (typical literature value for total skin capacitance). Frequency = 0.1 Hz. Observe the very small area inside the curve and the symmetry across the voltage axis.

significant phase difference was not apparent in the I *vs* V plots. The vertical distance between 2 points at the same voltage was taken as an estimate of the magnitude of hysteresis.

In 100% Cl^- Ringer and 0.1 Hz both voltage and current *vs* time and I *vs* V relations (Figure 6A and B) showed considerably lower phase differences (in A) and rectification and hysteresis (in B), respectively, in comparison with 20% Cl^- Ringer at the same frequency. The curve approaches the instantaneous current responses to voltage pulses (at 100% Cl^-) and indicates a "smearing" effect of high [Cl^-] on the voltage modulation of Cl^- permeability.

In the absence of Cl^-, the skin conductance dropped appreciably, but there still remained a certain degree of hysteresis in the I *vs* V curve (Figure 7C).

Discussion

Figure 1 summarizes the main elements of the present discussion. R_{apical} is assumed to be a function of apical P_{Cl} which is voltage dependent. $R_{basolateral}$ is taken as constant. C_{apical} and $C_{basolateral}$ are assumed to be voltage independent and constant.

The rectification seen in the current *vs* voltage curves, best evidenced at $[Cl^-]$ = 23.4 mM (Figure 3C), indicates that the voltage modulation of apical Cl^- permeability contains both fast and slow components.

With the apical membrane depolarized by transepithelial short-circuit and high-$[K^+]$ Ringer, apical Cl^- channels should be in a state of quasi-maximal Cl^- permeability activation (9,10,19). This probably explains why there is no significant increase of current after the fast initial current spike following a negative pulse. In contrast, negative pulses in symmetrical NaCl Ringer (9) generate a negligible initial current response (following the voltage pulse) with a subsequent sigmoidal increase of current with time. The comparison of the responses to negative pulses in KCl (present paper) and in NaCl Ringer (9) suggests that the fast current response to negative pulses in 20% $[Cl^-]$ K^+ Ringer simply reflects the ohmic response of the skin in a high Cl^- permeability state of the apical membrane of the MR-cells.

The relaxation curves observed in response to the -100 to zero mV maneuver indicate the reversal of an ion-cumulative process, the most likely explanation being Cl^- ions exiting the MR-cells through the apical membrane and with K^+ ions leaving the cell through the basolateral membrane (21). Similar relaxation currents have been documented by Larsen (9) minus the fast spike. This suggests that the integral area under the relaxation current *vs* time curve would then be proportional to the amount of charge accumulated in the MR-cells during the negative pulse. It is interesting to note that in 100% Cl^- Ringer the relaxation currents are negligible. This may be due to the fact that, under this condition, MR-cells are already maximally loaded with Cl^- ions (21) during the short-circuit basal state, thus receiving very little Cl^- uptake with the negative pulse.

The possibility that the current transients that follow most voltage steps are due to capacitive artifacts cannot be ruled out *a priori*. However, if this were the case, these currents should relax to zero in a few milliseconds, being detected as "instantaneous" on the time scale used by us. Additionally, there is no evidence of capacitive artifacts in 100% Cl^- Ringer (Figure 2C) which is a strong argument against a capacitive nature for this transient current, despite the fact that Schoen and Erlij (22) measured capacitive transients up to 600 ms. Also, the possibility of fast ionic profile shifts causing the observed transients cannot be ruled out. Against this last possibility is the fact that the transients became unimportant in either 100% or 0% Cl^- Ringer, thus implying ionic specificity and concentration dependence.

The marked (although partial) conductance inactivation caused by positive apical voltages fits the general idea that the Cl^- conductance of the apical membrane of MR-cells is quiescent when the cytoplasm is significantly negative with respect to the apical solution (9). High positive apical voltages in the high $[K^+]$-depolarized preparation most probably mimic the apical voltage profile prevailing in symmetrical NaCl Ringer in which the cytoplasmic voltage is significantly negative in relation to the external side, and in which the apical Cl^- permeability is minimal (9,19). Evidence of this low apical Cl^- permeability is seen both in the graphs of current *vs* time and in the I *vs* V relations at 20% Cl^- Ringer, with increasing positive voltages (Figures 2B and 3C, respectively). The rectification observed at positive voltages was established as early as within 600 ms (Figure 3C), contrary to the view proposed by Larsen (9) who has con-

sidered this inactivation, as well as its reversal, as intrinsically slow phenomena.

The fast and slow components of the current inactivation in response to positive pulses may be explained by the action of the cytoplasm-directed electric field across the apical membrane of MR-cells which inactivates apical Cl^- channels in a way that is essentially fast (19). What is seen as a slow component of the inactivation process is possibly the result of the gradual build-up of voltage across the apical membrane, according to the scheme below.

The fraction of the total voltage falling across the apical membrane after a positive transepithelial pulse gradually increases with time, as the apical membrane becomes less and less conductive due to the inhibitory effect of the positive voltage, constituting a positive feedback loop for inactivation by voltage. The less conductive the apical membrane becomes, the larger is the fraction of voltage falling across it, a fact that makes the apical membrane even less conductive, closing the loop.

Positive apical voltages lose most of their inhibitory effect in 100% Cl^- Ringer (Figure 2C). It seems that the Cl^--conductive pathway, constituting most of the skin conductance under these conditions, is refractory to voltage at high $[Cl^-]$. A high $[Cl^-]$ apparently counteracts the skin conductance inhibition brought about by apical positive voltages. This effect is observed both in the instantaneous I *vs* V curves and in the current responses to sinusoidal voltages.

Apical membrane hyperpolarization, with cytoplasmic negativity, is achieved with the +100 mV pulses. This condition seems to inactivate apical P_{Cl} with apparent kinetics of several seconds. Pulse clamping to zero from +100 mV, however, relieves this inhibition with a much faster kinetics of about 100 ms.

As mentioned above, low cytoplasmic Cl^- concentration leads to inactivation of apical P_{Cl} (10), and conditions associated with high cytoplasmic Cl^- concentration are often of high Cl^- permeability. Under our "basal" conditions (short-circuit, $[K^+]$ = 117 mM and $[Cl^-]$ = 23.4 mM), the apical membrane is depolarized and $[Cl^-]_{cell}$ is presumably high. This favors apical P_{Cl} activation, as demonstrated by a large current response to pulsing the skin voltage to either sign. When the skin is rapidly clamped from short-circuit to -100 mV the apical membrane probably does not get the full share of the total applied voltage due to its high conductivity in the previous short-circuit condition. Also, the transapical voltage under -100 mV clamping favors P_{Cl} activation by a double-barreled effect: Cl^- ions are kept inside the cell by the electric field at the same time that the voltage signal favors, by itself, apical P_{Cl} activation.

In going from short-circuit to +100 mV a different combination of effects takes place. The cell now tends to lose Cl^- ions due to increased cytoplasmic negativity. Concomitantly, the apical membrane gradually polarizes leading to P_{Cl} inactivation by voltage. Now, both apical polarization and Cl^- depletion pull in the same direction, such as inhibiting apical P_{Cl}. Due to the progressive increase of the apical membrane electrical resistance (caused by apical P_{Cl} inactivation and decreased $[Cl^-]_{cell}$) the applied voltage rapidly builds up mostly across the apical membrane. This combination of factors leads to intense conductance inactivation demonstrated experimentally by the marked current decrease.

On the basis of these considerations, the findings in the pulse combination protocol can be explained as follows: at sustained -100 mV the MR-cells are maximally loaded with Cl^- which, combined with activating apical voltage, creates maximal apical Cl^- permeability. Pulse inversion from this condition occurs at maximal skin conductance, seen as a fast and significant current response to the applied +100 mV. A relatively slow (500 ms) but important current inhibi-

tion then takes over, in which the sequence discussed above inserts.

Since apical conductance is significantly inhibited at sustained +100 mV, in this situation the skin potential difference falls mostly over the apical membrane and is immediately released from this location when the potential difference changes sign.

Voltage clamping to +100 mV (from sustained -100 mV) generates a current response which is typically 1.5 times larger than the steady-state current at -100 mV. This may be explained by the superposition of the relaxation (diffusionally driven) current observed at clamping to zero from -100 mV, intensified by the positive voltage. However, the effect is not symmetrical, since from +100 to -100 mV the increase is not observed. This raises the interesting possibility that a hidden activation is present in the -100 mV situation, in the sense that the activating effect of negative voltage cannot manifest during the -100 mV clamping, but reveals itself when the skin is brought to +100 mV. We cannot presently test this possibility.

As mentioned above, upon going directly from +100 to -100 mV, after a few seconds of conditioning at +100 mV, there is an instantaneous release of the voltage inhibition seen at +100 mV. This observation is difficult to reconcile with the existing idea of a slow voltage modulation of the apical Cl^- permeability (9). If we consider, however, the possibility that inactivation/release of apical P_{Cl} by a cytoplasm-directed electric field is essentially fast then it makes sense that, upon instantaneous release of this inhibitory field, the apical Cl^- channels immediately recover from the inhibition caused by previous conditioning at +100 mV. As such, the "memory" of inhibition by voltage appears to be of very short duration.

Comparing the current responses to slowly varying sinusoidal voltages in 20% Cl^- Ringer at 0.1 Hz with the recovery from positive voltage steps, it becomes apparent that recovery from the inhibition brought about by the positive voltage returns slowly in a sinusoidal stimulation, but the recovery is considerably faster (about 100 ms) when the +100 mV pulse is suddenly brought to zero or reverted to -100 mV.

The last result indicates that not only the magnitude and signal of the voltage do play a role in the modulation of Cl^- channels but the rate of voltage change with time is important as well. This line of reasoning indicates that fast voltage changes are more efficient in eliciting the corresponding inhibitory or releasing effect of Cl^- permeability. For example, at the frequency of 0.02 Hz there should be no apparent hysteresis since at that low dV/dt rate there should be sufficient time for the conductance to adapt to the new voltages continually being fed to the skin. Figure 7A shows, however, hysteresis even at 0.02 Hz. This suggests that, when dV/dt is low, the recovery from the inhibitory positive voltages is proportionally slow.

In the voltage step protocols, for example, changes from +100 to -100 mV are fast (10 ms at most). Leaving out the first 600 ms (where capacitance artifacts might be involved (22)) it is clear from Figure 4B that the skin regains, in a fraction of a second, the conductance prior to the +100 mV maneuver. On the other hand, when the voltage is brought slowly (in sinusoidal form) from +100 to -100 mV the current follows a return pathway clearly distinct from the ongoing -100 to +100 mV one, indicating a more persistent memory of the inhibiting positive voltage (Figure 5A).

Another way we looked at hysteresis (as opposed to the *recovery time* point of view) was on the basis of the time it takes for the voltage inactivation of Cl^- permeability to proceed. Hysteresis along the positive voltage axis would then be a result of the fact that, upon returning, the positive voltage has not yet totally accomplished the inactivation of Cl^- permeability so that further inactivation continues to develop along the returning pathway. This observation is in accordance

with the finding that the inhibition brought about by a positive voltage develops slowly.

Another feature already pointed out above is the fact that, even at the higher frequency of 1 Hz at 23.4 mM [Cl^-], there is essentially no phase difference between current and voltage (Figure 7B) since the maximum value of positive voltage falls only slightly to the right of the maximum current value. On the negative side of the voltage axis minimum values of current and voltage exactly coincide.

Comparing the I *vs* V curves taken for 23.4 and 117 mM [Cl^-] Ringer the hysteresis is negligible in the latter situation. This fact further reinforces the view that the observed hysteresis is not due to a capacitive impedance since it is difficult to explain how the capacitance of the skin should be so importantly dependent on the particular composition of a solution. Also, on both the ongoing and returning portions of the curve the currents at zero voltage are negligible in 117 mM [Cl^-] Ringer. An interesting fact is that the I *vs* V curves obtained with sinusoidal stimulation coincide perfectly during many cycles (data not shown).

In the simulation of the skin electric behavior we used a parallel RC (resistance capacitance) circuit in a computer program (see Appendix, Equation 1 and Figure 7D) with R = 406 ohm (typically measured skin value in 23.4 mM Cl^- Ringer) and C = 100 microFarad (estimated value from the literature (22)). The generated curve (Figure 7D) differs completely from the experimental one (Figure 5B), indicating that the experimental curves can be explained only if one assumes that skin resistance varies with time and voltage in the presence of sinusoidal stimulation.

Appendix - Current across a parallel RC circuit driven by a sinusoidal voltage. The following equation is derived from Ref. 23:

$$I(t) = E_0 \left\{ \frac{1}{R^2} + (\omega C)^2 \right\}^{1/2} \cos(\omega t + \arctan(R\omega C))$$

where E_0 = 0.1 volt. *I(t)* is the current at any given time t, R is the resistance, C is the capacitance and ω is the angular frequency in radians x s^{-1}.

References

1. Bruus KP, Kristensen P & Larsen EH (1976). Pathways for chloride and sodium transport across toad skin. *Acta Physiologica Scandinavica*, 97: 31-47.
2. Katz U & Scheffey C (1986). The voltage-dependent chloride conductance of toad skin is localized to mitochondria-rich cells. *Biochimica et Biophysica Acta*, 861: 480-482.
3. Larsen EH (1982). Chloride current rectification in toad skin epithelium. In: Zadunaisky JA (Editor), *Chloride Transport in Biological Membranes*. Academic Press, New York, 333-364.
4. Larsen EH & Kristensen P (1978). Properties of a conductive chloride pathway in the skin of the toad (*Bufo bufo*). *Acta Physiologica Scandinavica*, 102: 1-21.
5. Larsen EH & Rasmussen BE (1982). Chloride channels in toad skin. *Philosophical Transactions of Royal Society of London, Series B: Biological Sciences*, 299: 413-434.
6. Larsen EH & Rasmussen BE (1983). Membrane potential plays a dual role for chloride transport across toad skin. *Biochimica et Biophysica Acta*, 728: 455-459.
7. Larsen EH & Rasmussen BE (1985). A mathematical model of amphibian skin epithelium with two types of transporting units. *Pflügers Archives*, 405 (Suppl 1): S50-S58.
8. Larsen EH, Ussing HH & Spring KR (1987). Ion transport by mitochondria-rich cells in toad skin. *Journal of Membrane Biology*, 99: 25-40.
9. Larsen EH (1991). Chloride transport by high-resistance heterocellular epithelia. *Physiological Reviews*, 71: 235-283.
10. Procopio J & Lacaz-Vieira F (1990). Roles of external and cellular Cl^- ions on the activation of an apical electrodiffusional Cl^- pathway in toad skin. *Journal of Membrane Biology*, 117: 57-67.
11. Voute CL & Meier W (1978). The mitochondria-rich cell of frog skin as hormone sensitive "shunt path". *Journal of Membrane Biology*, 40: 141-165.
12. Willumsen NJ & Larsen EH (1986). Membrane potentials and intracellular Cl^- activity of toad skin epithelium in relation to activation and deactivation of the transepithelial conductance. *Journal of Membrane Biology*, 94: 173-190.

13. Alvarado RH, Dietz TH & Mullen TL (1975). Chloride transport across isolated toad skin of *Rana pipiens*. *American Journal of Physiology*, 229: 869-870.
14. Foskett KJ & Ussing HH (1986). Localization of chloride conductance to mitochondria-rich cells in frog skin epithelium. *Journal of Membrane Biology*, 91: 251-258.
15. Katz U, Van Driessche W & Scheffey C (1985). The role of mitochondria-rich cells in the chloride current across toad skin. *Biology of the Cell*, 55: 245-250.
16. Lacaz-Vieira F & Procopio J (1988). Comparative roles of voltage and Cl ions upon activation of a Cl conductive pathway in toad skin. *Pflügers Archives*, 412: 634-640.
17. Biber TUL, Walker TC & Mullen TL (1980). Influence of extracellular Cl concentration on Cl transport across isolated skin of *Rana pipiens*. *Journal of Membrane Biology*, 56: 81-92.
18. Mandel LJ & Curran PF (1972). Chloride flux via shunt pathway in toad skin: Apparent exchange-diffusion. *Biochimica et Biophysica Acta*, 282: 258-264.
19. Larsen EH & Harvey BJ (1994). Chloride currents of single mitochondria-rich cells of toad skin epithelium. *Journal of Physiology*, 478: 7-15.
20. Klemperer G, Garcia-Diaz JF & Essig A (1986). Basolateral membrane potential and conductance in frog skin exposed to high serosal potassium. *Journal of Membrane Biology*, 90: 89-96.
21. Spring KR & Ussing HH (1986). The volume of mitochondria-rich cells of frog skin epithelium. *Journal of Membrane Biology*, 92: 21-26.
22. Schoen HF & Erlij D (1985). Current-voltage relations of the apical and basolateral membranes of the frog skin. *Journal of General Physiology*, 86: 257-287.
23. Purcell EM (1965). *Electricity and Magnetism*. *Berkeley Physics Course*. Vol. 2. McGraw-Hill Book Co., New York.